Iranian Polymer Journal (2020) 29:1099–1112
https://doi.org/10.1007/s13726-020-00864-y

ORIGINAL RESEARCH

Impact of inclusion of graphene oxide nanosheets on polypropylene thermal characteristics

Maziyar Sabet[1] · Hassan Soleimani[2] · Erfan Mohammadian[3,4] · Seyednooroldin Hosseini[5]

Received: 7 January 2020 / Accepted: 7 September 2020 / Published online: 15 September 2020

Abstract

Thermal steadiness and flame-resistant characteristics of PP/GO nanocomposites were explored. Inclusion of graphene oxide nanosheets (GOs) increased thermal steadiness of the nanocomposites by at least 50 °C through nano-confinement of PP connections and restriction of release of gaseous molecules during degradation. Pyrolysis showed that process of the degradation of PP was not changed in the presence of nanofillers and alkenes consisting of carbon particles that were deterioration products. With addition of GOs to PP, cone calorimetry experiments exposed a substantial deviation in ignition under irradiation. In addition, inclusion of GOs reduced PP's rate of combustion owing to the creation of a carbon shielding sheet acting as the heat and mass transfer barrier. Uniformly dispersed GOs shifted the decomposing onset temperature (T_{onset}) of PP to around 40 °C higher which induced a great melt flow rate in the composites and dramatically changed their fire behavior. Delayed dripping resulted in considerably enhanced heat absorption and reduced time for ignition. As a result of development of a shielding film in combustion, under flaming conditions, the highest thermal discharge level of 78% was accomplished. The most prominent features that made PP to prefer carbon nanoparticles were demonstrated by the well-exfoliated GO nanosheets in the PP matrix which was evidenced by TEM images. Findings of TGA indicated that the GO's addition enhanced the thermal steadiness and PP's char yields. The nanocomposites of PP/GO 5.0 wt% attained UL-94 with a grade of no dripping and grade V-1. Cone calorimeter test results showed that the PP's burning performance, peak heat release rate (PHRR) and average specific extinction area decreased noticeably when the GOs' combination effects was intervened. PHRR showed a decrease of 46% compared to the neat PP for the PP/GO 5.0 wt% nanocomposite. This role offered a new modified approach to enhance the GO's flame-resistant effectiveness.

Keywords Graphene oxide · Polypropylene · Thermal stability · Flammability · Thermal characteristics

Introduction

Polypropylene (PP) is one of the widely used polyolefins which quickly catches fire and melts when exposed to fire. Therefore, improving its thermal stability and flame-retardant properties are of the first-rate importance [1–3]. Halogenated flame-resistant materials are no longer permitted to be utilized due to environmental and health issues [4]. Halogen-free flame-resistant, particularly intumescent flame-resistant, has attracted significant attentions in the growth of high-performance PP nanocomposites owing to the exceptional benefits, for example, low smoke and toxic gas yields, and halogen-free characteristics [5].

Utmost, polymeric nanocompounds do not generally put out and burn gently up to burning all the fuel is burned [6]. The intumescent flame-resistant additive is considered to be a promising halogen-free flame-resistant additive for

✉ Maziyar Sabet
maziyar.sabet@utb.edu.bn

[1] Peroleum and Chemical Engineering, Universiti Teknologi Brunei (UTB), Jalan Tungku Link, Mukim Gadong A, Bandar Seri Begawan BE1410, Brunei Darussalam

[2] Department of Fundamental and Applied Sciences, Faculty of Science and Information Technology, Universiti Teknologi PETRONAS (UTP), Persiaran UTP, 32610 Seri Iskandar, Bandar Seri Iskandar, Ipoh, Perak, Malaysia

[3] Faculty of Applied Sciences, Ton Duc Thang University, Ho Chi Minh City 700000, Vietnam

[4] Department for Management of Science and Technology Development, Ton Duc Thang University, Ho Chi Minh City 700000, Vietnam

[5] Department of Petroleum Engineering, EOR Research Center, Omidiyeh Branch, Islamic Azad University, Omidiyeh, Khuzestan, Iran

environmental concerns attributable to the benefits of low toxicity and elevated flame-retardant effectiveness [7]. The prominent flame-resistant mechanism of intumescent flame-resistant is the formation of a swollen multicellular charred layer on the surface, producing a physical protective barrier [8]. It is noticeable to know that the loading of regular macro flame-retardants such as magnesium or aluminum hydroxides is extensively huge and may reach 40–65 wt% of the whole compound content and even higher which weakens the mechanical properties of the polymers [9–11].

By comparison with the other halogen-free flame-retardants, such as carbon nanotubes or layered hydroxides, graphene oxide (GO) can cover the exterior surface of the polymer with a strong sticky intumescent char, that has a lower density but the more efficient protection [12–14].

Nanotechnology's aim in the production of the polymer flame-resistance is recognized as a revolutionary approach. By adding a tiny quantity of nanofiller, the flame-retardants of the polymer can be considerably improved. Low loading of graphene oxide (GO) resulted in the significant improvement in the thermal steadiness, mechanical characteristics, and thermal and electrical conductivities of the polymer nanocomposites [15].

Moreover, GO is used as a promising flame-resistant polymer nanofiller, including charring and non-charring materials. The mode of action of GO for increasing the flame retardancy of PP has been usually recognized by the hindrance impact of the carbon nanomaterial residue that results in a restriction of the heat and mass transfers between gas and condensed phases [16]. Furthermore, the char's barrier efficiency was strengthened and thermal conductivity and diffusivity were altered by incorporation of the reduced graphene oxide (RGO) [17]. The GO inclusion would be expected to show a desirable impact on the values of the limiting oxygen index (LOI) and UL-94 compared to the halogenated flame-resistant PP composites [18].

GO operates as a flame-resistant nano-filler for polymers because of its two-dimensional morphology, high aspect ratio, and specific surface area [19, 20]. GO functioned to prevent the producing of the polymer pyrolysis gasses and as a physical hindrance for the transport of the heat and mass [21–23].

The LOI and UL-94 tests match the burning situation, and the experiment with cone calorimetry demonstrated combustion under the fire stage [24, 25]. The specimen was put horizontally in a sample holder for cone calorimetry, removing any physical impacts of the polymer burning, for example dripping [26–28]. Then, the impact of the protective layer was tested to identify the effectiveness of the GO flame-retardant properties [29].

Intumescent char formation took place through a semi-liquid stage coinciding with the gas discharge and char expansion [30–32]. Modifying physical and chemical characteristics could optimize flamed-resistant effectiveness [33–35]. The system's melt viscosity played a vital role in the effective intumescent char development [36–38]. When the viscosity was not very thick or very thin during polymer degradation, intumescent char formation was expedited [39–41]. If the viscosity of the degraded polymer be very small, gasses have not been detained, but rather spread to feed the flames [42–44], leading to bad intumescence. If viscosity be sufficient, the formation of an expanded structure would result in a slow diffusion [45, 46]. When the viscosity of carbonizing material be very high, the gasses were heavily detained and diffusion would be significantly suppressed, thus inhibiting the intumescence of the char [47, 48].

In cone calorimetry experiment, a slightly augmented viscosity produced by the low GO load was the reason for the extremely extended char. The impact of GO inclusion in the melt viscosity enhancement was recognized as a mechanism of anti-dripping [49–51]. However, the UL-94 test still identifies melt dripping of a polymer matrix, likely due to the retardation of the discharge of incombustible gases and formation of low-quality char [52–54].

Understanding the mechanism of thermal decomposition helps to improve the thermal steadiness of the polymer nanocomposites. Carbon-based nanomaterials such as carbon nanotube and C60 are generally considered to be eco-friendly materials with remarkable thermal characteristics, mechanical properties, and flame retardancy. The use of carbon family materials and their effectiveness as barriers in promoting the thermal stability of the polymers and inhibiting fire of flame-retardants has not been widely studied. In fact, C60 not only acts as the fortifiers for graphene and barriers, but also has a free radical trapping effect in polymeric matrices. As a result, the interaction of nano-filler and polymer matrices was effectively improved and mechanical properties of the PP-based composite were enhanced due to the free radical-trapping effect of the C60 and the thermal barrier effect of the graphene layers [55].

In the present work, the effects of inclusion of GO nanosheets on the behavior of burning and heat characteristics of PP were explored, which showed how GO can be used as a flame-resistant. Its incorporation resulted in various PP/GO nanocomposites that were responded to the small flame experiments and ignition under fire conditions. The intumescent flame-resistant comprised of PP and GO acted as carbonization. In the PP/GO flame-resistant materials, GO nanosheets were inserted and their impacts on the combustibility and heat discharge of the fire-resistant PP/GO nanocomposites were studied. The findings showed that GO inclusion could further decrease the PHRR value of the flame-resistant PP/GO materials. The charred composition, melt viscosity and hindrance impact of GO were contributed to various functions in improving LOI levels, UL-94 grading, and decrease of heat discharge. This work offered a

solution for the comprehensive assessment of the synergy or antagonism impacts of GO which benefits the development of its flame-resistant system as a reinforcement of the fire prevention and flame retarded polymer composite materials. The superiority of the GO is its shape, two dimensional and flat structure. The significance of this study for readers is the role of GO (up to 5.0 wt%) in boosting the fire security properties of the PP martials. The digital photo and cone calorimetry test of the fired PP/GO nanocomposite showed the development of the charred, cohesive and sticky intumescent that augmented the melt viscosity and performed as a barrier to protect people against toxic fumes and fire.

Experimental

Materials

Graphite flakes was acquired from Kropfmühl AG (RFL 99.5, Germany) and polypropylene (PP) homopolymer (Moplen HP501L) was supplied from LyondellBasell (Germany) with a flow index of 6.0 g/10 min and a melt density of 900 kg/m^3. All commercial chemicals were used as they were obtained without further purification.

Material processing

Single layer of graphene oxide (GO) was generated from extended graphite employing an improved method of Hummers and vacuum-dried under P_2O_5 at room temperature for a week [1–6]. PP was dried in vacuum oven at 80 °C overnight before use. PP/GO composites were prepared as follows: 3 g of GO powders was spread in 350 mL of toluene with the assistance of sonication for 35 min at room temperature. Afterward, 20 g of PP was added to the GO/toluene suspension and dissolved after mechanical mixing at 100 °C for 2 h. All PP/GO compounds were processed under the same scenarios. Typically, GO was distributed in acetone and combined with PP pellets; afterward vacuum removal and acetone elimination before melting. There were no additional compatibilizer. A co-rotating twin-screw extruder was utilized to inject resulting PP/GO powder blends at 210 °C. TEM was used to determine the morphology of the PP nanocomposites. Despite huge specific surface regions, the graphene-based products were distributed evenly.

Characterization

LOI was evaluated using an ASTM D2863-97 standard by a Jiangning (HC-2, China) oxygen index meter. Sample dimensions were $100\times6.7\times3$ mm^3. To achieve an average value, five samples were screened. The vertical burning experiment of UL-94 was performed using horizontal and vertical burning equipment, Jiangning (CZF-II, China) as per ASTM D3801. Sample sizes were $127\times12.7\times3$ mm^3. At least five times the experiments were repeated.

Scanning electron microscopy (SEM) micrographs were obtained at an acceleration voltage of 5 kV by a FEI Sirion 200 scanning electron microscope (The Netherlands). Transmission electron microscopy (TEM) was utilized to assess GO morphology in the PP polymeric structure. A drop of graphene ethanol distribution was dehydrated on the copper grid. Nanocomposite sheet was microtomed with a Cambridge ultratome to 20–100 nm thickness slices and then transmitted to the copper grid. TEM images were developed on a JEOL (JEM-2100F, Japan) microscope at 200 kV.

Experiments for thermogravimetric analysis (TGA) were conducted using an instrument (Setaram Setsys TG-DTA, France) 16/18, 5 ± 0.5 mg of the specimen was subjected into an alumina vessel and an empty vessel of alumina applied as a reference. Specimens were heated at 10 °C/min under a 50 mL/min flow of N_2 from room temperature up to 600 °C. To assess thermal steadiness of materials, sample mass, temperature, and heat flow were constantly documented. Onset temperature was described from 2% mass loss.

In an ISO 5660 FTT cone calorimeter (UK), the burning behavior under forced-flamming circumstances was explored. The rate of 35 kW/m^2 irradiation in the horizontal setup was employed for $100\times100\times3$ mm^3 specimens. Flame-out was defined as a visible yellow flame extinguishing. Total heat values (THE) evolved and the residue amount was drawn at flame-out, described as flaming burning prior residues were burned in the following afterglow.

Furthermore, fire residues at flame-out were separated from cone calorimeter and cooled with liquid nitrogen to prevent subsequent afterglow thermo-oxidation and thus residue structures produced throughout the combustion process. The residues of the chars were analyzed by SEM. A Nicolet spectrophotometer (6700, USA) in the wavenumber range of 4000–400 cm^{-1} was used to obtain Fourier transform infrared (FTIR) spectra. A LABRAM-HR laser confocal micro Raman spectrometer (France) provided with a laser source of 514.5 nm was used to measure the Raman spectra. A smoke density tester apparatus (Jiangning JSC-2, China) was used to explore the characteristics of smoke evolution in the scenario of flaming combustion according to ISO 5659-2.

Specimens with the $75\times75\times1$ mm^3 sizes were subjected to an outer flow of heat (35 kW/m^2) for pilot burner purposes. Melt flow index (MFI) was determined with a heavy weight of 2.16 kg at varying temperatures via a melt flow stream apparatus (GB3682-2000 SRZ-400C, China).

Table 1 LOI and UL-94 test results for neat PP and PP/GO nanocomposites

Tests	Specimen code				
	PP	PP/GO 0.5 (wt%)	PP/GO 1.0 (wt%)	PP/GO 2.0 (wt%)	PP/GO 5.0 (wt%)
UL-94UL-94					
Rating	NR	V-0	V-0	V-0	V-1
Dripping	Yes	No	No	No	No
LOI (%)	18.7 ± 1.0	18.5 ± 1.0	18.1 ± 1.0	18.0 ± 1.0	17.7 ± 1.0

Results and discussion

Vertical flammability experiments assessed the flammability of the nanocomposites and compared the outcomes with those of the pristine PP. As anticipated, there was fast and complete combustion in the PP matrix, along with rigorous dripping from the samples. The inclusion of GO did not lead to a significant decrease in the flammability of PP as no self-extinguishment was detected for nanocomposites and all PP/GO specimens stopped dripping, proposing a substantial decrease in burning level and existence of nanoparticles.

Table 1 presents the flammability characteristics of PP and PP/GO specimens with different proportions of GO in regards of LOI and UL-94 tests. In the UL-94 experiment, PP received an 18.7 ± 1.0 vol% LOI with no rating (NR) grade. The addition of different carbon nanomaterials, respectively, resulted in no or only slight improvement in the response of the polymers to the small flame. Pristine PP is highly flammable and has an LOI rating of 18.7 ± 1.0 vol%, and failes the UL-94 experiment. The findings of LOI and UL-94 tests examined the influence of GO content on the nanocomposites flame-retardancy. In other words, in the case of the LOI test, GO's incorporation in the PP/GO nanocomposites did not influence on the LOI values and did not support flame-retardant enhancement and statistically remained unchanged.

The LOI results showed that the surface of PP/GO nanocompounds is not protected by GO inclusion before the intumescent barrier layer formation. However, the UL-94 experiment findings supported the outcomes of cone calorimeter tests, indicating that the addition of GO developed flame-retardancy of the PP/GO nanocomposites. The UL-94 rating of the PP/GO specimens was promoted to V-1 compared to that of the pristine PP, which showed that the graphene mixture played a significant role in improving the PP system's flame-retardants. The flame-retardant results showed that GO can improve the UL-94 level, but it has no remarkable effect on the LOI value. To date, there has been a lack of systematic research on the impacts of GO on the combustion, expansion behavior, structure and decomposition processes.

TGA-DTG tests under nitrogen (Figs. 1, 2) assessed the thermal steadiness of the nanocomposite specimens. The presence of GOs significantly delayed the thermal

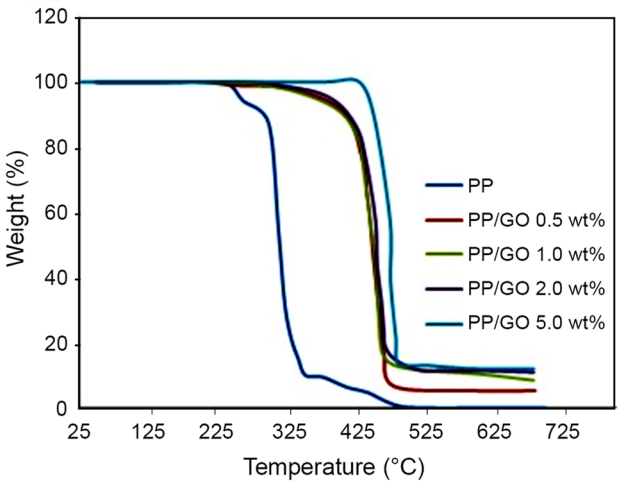

Fig. 1 TGA curves of neat PP and PP/GO nanocomposites

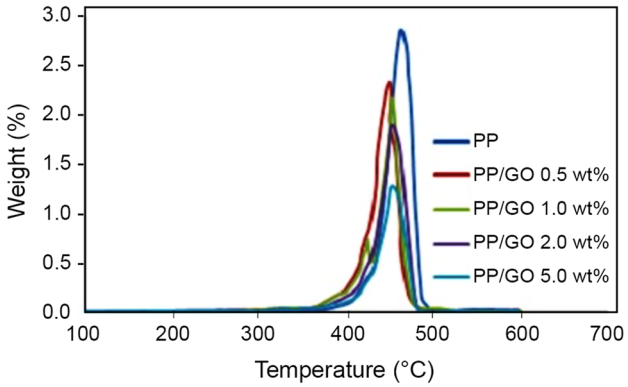

Fig. 2 DTG curves of neat PP and PP/GO nanocomposites

degradation for all GO loadings, while maximum improvement in thermal steadiness happened once the matrix was strengthened with 5.0 wt% GO, increasing the onset degradation by 150 °C. GO is a thermally unstable material corresponding to the elimination of functional labile oxygen groups [25], but the impact of GO resulted in postponing of the thermal degradation of PP/GO nanocomposites.

The geometric characteristics of GOs (with an enormous aspect ratio and surface area) considerably improved thermal steadiness for all samples and recognized that GO addition

developed interactions, tortuous path formation and restriction of gaseous molecules release throughout the thermal breakdown. The findings can be regarded in relation to the notion of nano-confinement [31], according to which the presence of GO produced regions, where the matrix's macromolecular connections were restricted, disturbing their periodic coil conformation and limiting their motion.

This experience proved the elevated thermal steadiness of the samples as GO nanosheets occupied a wide range of regions in the sample volume, formed a well-dispersed filler network that confined the PP macromolecules motion even more. The results showed that the highest increase in the PP's thermal steadiness happened at the first level of GO inclusion (0.5 wt%) compared to the higher GO inclusions (1.0–5.0 wt%). Under an inert atmosphere, the thermal decomposition of the polymer was strongly correlated to its retardant flame. Within 360–495 °C pristine PP was decomposed and no apparent residual mass was remained.

The nanocomposites of PP/GO displayed a comparable behavior of decomposition with the neat sample. The addition of GO had a negligible impact on the PP nanocomposites heat of decomposition, including the weight loss phase and remained chars. The inclusion of GOs changed the shape of the shoulder from peak to weak. This can be ascribed to GO nanosheets barrier efficiency, reduced the propagation of the degradation products. The temperature of weight loss of 5 wt% was the temperature at which the nanocomposites begun to break down (T_{onset}) and the temperature at which the weight loss reached its limit was set to T_{max}. Primary degradation temperature (T_{onset}) described as the 5 wt% weight loss temperature and the highest degradation temperature (T_{max}) were obtained from DTG curves.

In the N_2 atmosphere, the T_{onset} for the nanocomposites was higher than the pristine PP. For instance, with 2 wt% GO, the highest enhancement in T_{onset} was achieved at 385 °C. This increase in thermal steadiness can be ascribed mainly to the GO physical barrier that efficiently stopped releasing of the volatile degradation products [36].

Under the N_2 condition, however, there is little increase in T_{max} for the nanocomposites. In addition, the remaining mass of PP/GO nanocomposites in the N_2 atmosphere was significantly enhanced by the inclusion of GO compared with the pristine PP. PP and its nanocomposites displayed one-step pyrolysis under N_2 atmosphere, corresponding to polymer backbone thermal degradation.

The thermal steadiness of PP/GO nanocomposites was comparable to that of the pristine PP from the nitrogen-based TGA analysis. In addition, PP/GO nanocomposites remaining weights were higher than that of the pristine PP. However, PP/GO's thermal steadiness was significantly improved. For instance, PP/GO's T_{max} was 150 °C higher than that of the pristine PP. Powerful interfacial interactions among nanofillers and polymer matrix improved the nanocomposites' heat degradation activation energy by limiting the thermal movement of the polymer connections [40]. GO's charring impact was accountable for the PP/GO nanocomposites reduced thermal steadiness and increased char yield [11].

Amazingly, the 5.0 wt% GO inclusion in PP raised the remaining char from 0.55 to 12.56 wt%. Nanocomposites' enhanced char yield means that part of the polymer matrix was not fully combusted, resulting in increased flame retardation. Due to the physical barrier impact of well-spread GO on the release of volatile decomposition products; it is evident from the DTG analysis that the maximum mass-loss rate of the nanocomposites were reduced with GO addition.

Pristine PP breaks down at 260–350 °C quickly and is exhausted at higher than 495 °C without any remaining chars. However, nanocomposite PP/GO 5.0 wt% postponed the T_{onset} by 150 °C (Table 2). These findings are due to the impacts of GO platelet structures on the thermal insulator.

Under these experimental circumstances, intumescent flame-retardant PP/GO nanocomposites had comparable heat oxidative behavior. Though, it was noted that the remaining weights of PP/GO nanocomposites were higher than those of the pristine PP which means that for intumescent flame-retardant PP/GO nanocomposites more residual chars were acquired than for the pristine PP (Fig. 2). In the meantime, T_{onset} and T_{max} of the PP/GO specimens were increased by 150 °C and 180 °C compared to those of the pristine PP, respectively. It shows that the mixing of PP/GO 5.0 wt% increased its thermal steadiness. On the other hand, the addition of 5.0 wt% graphene increased the PP T_{max} by 180 °C, indicating that the GO mixture has a strong thermal-increasing impact on the PP/GO structure in a high-temperature area. Enhanced char yield of nanocomposites means that

Table 2 TGA data of PP and its composites under N_2 atmosphere

Parameter	Specimen code				
	PP	PP/GO 0.5 (wt%)	PP/GO 1.0 (wt%)	PP/GO 2.0 (wt%)	PP/GO 5.0 (wt%)
T_{onset} (°C)	260 ± 5.0	355 ± 5.0	370 ± 5.0	385 ± 5.0	435 ± 5.0
T_{max} (°C)	460 ± 5.0	503 ± 5.0	518 ± 5.0	606 ± 5.0	649 ± 5.0
Residue %	0.0 ± 1.0	5.3 ± 1.0	11.5 ± 1.0	12.5 ± 1.0	13.3 ± 1.0

T_{onset} onset degradation temperature (temperature at 5% weight loss), T_{max} maximum weight loss temperature

part of the polymer matrix was not fully combusted, which resulted in an increased flame-retardancy.

Table 2 shows the onset degradation temperature, maximum weight loss temperature and the percentage of the residue specimen after burning. A closed and stable residue surface on top of the burning specimen is necessary for the function and effectiveness of the carbon nanomaterial residue to serve as a heat shield and barrier against mass transport. This protective layer can postpone the heat transport from the flame into the materials, resulting in a slower increase of temperature in the nanocomposite [44]. Table 2 displays that the percentage of residues, the values of T_{onset} and the T_{max} increased with GO inclusion. Consequently, GO inclusion has an effective role in boosting the thermal stability of the PP/GO nanocomposites.

The cone calorimetry is commonly utilized for studying materials' fire behavior in a laboratory scale. Cone calorimeter is planned to derive oxygen usage level into the heat release rate (HRR) throughout the burning of polymers according to the well-known concept of oxygen intake. To quantitatively assess fire behavior, many significant parameters, for example, peak heat release rate (PHRR), total heat release (THR) and ignition time (TTI) are reported.

Figures 3 and 4 display specimen heat release rate (HRR) and THR graphs at a heat flux of 35 kW/m^2 and the related data can be found in Table 3. Pristine PP burns heavily with a severe HRR peak (1140 kW/m^2) after ignition. Impressively, the inclusion of 0.5 wt% GO resulted in more decrease in PHRR, which for PP/GO sample, it lowered from 1140 kW/m^2 for PP to 970 kW/m^2, showing the superior hindrance efficiency of GO nanosheets for intumescent char.

It is evident that in PP/GO nanocomposites, combustion time among two peaks slowly reduced as GO loading increased. This is due to the improved thermal conductivity of the PP through the superior thermal conductivity of the

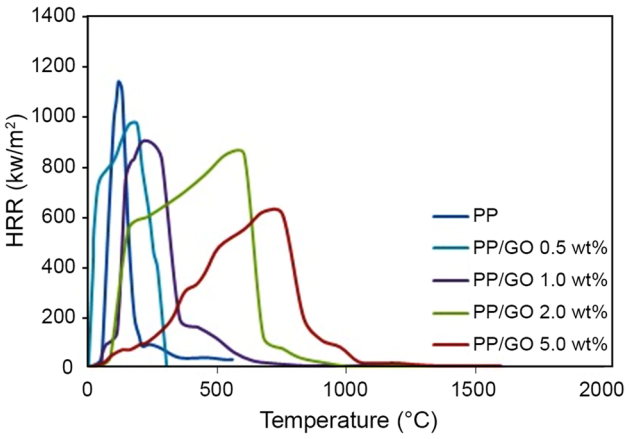

Fig. 3 Heat release rate variation of neat PP and PP/GO nanocomposites vs. temperature

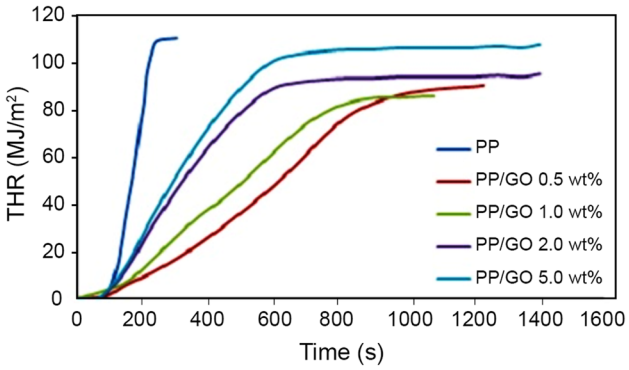

Fig. 4 Total heat release variation of neat PP and PP/GO nanocomposites vs. time

filler. While the inclusion of GO was 1.0 and 2.0 wt%, PHRR quantities of the relevant nanocompounds were reached to 936 and 880 kW m^{-2}, correspondingly. This evidence suggests that the flame-resistant efficiencies are not compatible with the sum of the GO inclusion, and the rate of synergistic effects at lower GO load was more effectively achieved; however, at higher graphene incorporation, the trend of un-flammability enhancement was still improved. Noticeably, the PP/GO 0.5 wt% THR value was further reduced to 86.0 MJ/m^2, smaller than that of the pristine PP.

The derived factors, for example, a fire growth index (FGI), delivered significant data about the fire hazards of polymeric materials. FGI is a ratio of PHRR and time to reach PHRR (TPHRR) [39]. Therefore, a greater FGI value implies a faster time to reach PHRR and an extra severe fire hazard [40]. A large reduction in FGI values was monitored for the PP/GO nanocomposite with 0.5 wt% GO inclusion compared to that of the pristine PP, which shows a great fire safety.

Meanwhile, the reduction in FGI values was continued with further GO incorporation. It can be concluded that GO's optimal load to enhance PP's fire safety was 0.5 wt% and further enhanced GO's load was detrimental to flame-resistant characteristics. Adding GO to PP significantly reduced the FGI. The PP/GO nanocomposite has the smallest FGI value, showing the highest performance among flame-retardants. GO's inclusion significantly improved PP's char yield. GO's excellent distribution outcomes, together with the marked flame-retardants, have an important barrier effect on the transfer of mass and heat.

An interesting remark came from the research described in Table 3 of the TTI attributed to PP and its nanocomposites. From all TTI results, as GO load increased, the TTI value decreased, which means the time to ignition was reduced when the GO load was high. This shows that GO inclusion can reduce the ignition delay time before the protected intumescent layer forms. This reality is particularly

Table 3 Cone calorimetry results of neat PP and PP/GO nanocomposites

Specimen code	TTI (S)	PHRR (kW/m^2)	ASEA (m^2/kg)	AMLR (g/s)	THR (MJ/m^2)	TSR (m^2/m^2)	FGI (kW/m^2.s)	T_{max} (S)	Residue (wt%)
PP	49	1140	552	0.049	118.4	600	5.70	200	0.5 ± 0.5
PP/GO 0.5 wt%	41	970	529	0.049	86.0	373	4.41	220	1.5 ± 0.5
PP/GO 1.0 wt%	39	936	511	0.048	90.4	375	3.90	240	2.1 ± 0.5
PP/GO 2.0 wt%	36	880	474	0.048	94.4	377	3.20	275	3.14 ± 0.5
PP/GO 5.0 wt%	30	620	357	0.046	96.0	380	2.10	295	3.9 ± 0.5

FGI = PHRR/t_{max} (fire growth index), *ASEA* average specific extinction area, *AMLR* average mass loss rate, *TSR* total smoke release, *THR* total heat release, *TTI* time to ignite

interesting, since nanocomposites were stated to be ignited sooner than the neat polymers [18, 38, 39]. The TTI of polymers is based on a variety of activities, such as heat transfer through monitoring the degradation responses of the heated polymer, determining volatile fuel release, and volatile mass transfer to the atmosphere. TTI test actually reports the smallest concentration of volatile material that is required, that a continuous flame can be established.

GO inclusion can obviously influence several ignitions controlling chemical and physical parameters, such as parameters of radiative absorption/release, thermal conductivity, heat capacity, and molten phase viscosity. In addition, postpone towards greater TTI can be anticipated at comparatively elevated inorganic loadings, merely linked to the reduced quantity of polymer available as the volatile fuel supply. Moreover, in the pre-ignition stage that is beyond the scope of this investigation a full description of the phenomenon explaining TTI interruption would involve the comprehensive characterization of these parameters.

The heat discharge level outline for pristine PP (Table 3) is normal for an extremely flammable, non-charging material, showing the full polymer volatilization and quick burning, yielding PHRR at 1140 kW/m^2 and flameout at about 200 s. Implementation of the GOs changed the phenomenology throughout the polymer combustion, resulting in a strong char production that influenced the shape of HRR analysis and decreased PHRR to nearly half of that, with GO level of 5.0 wt%.

Since combustion heat was discharged at a much-reduced pace, the contribution of PP/GO nanocompounds to a growing fire's development was considerably smaller than that of the pure PP, with apparent advantages in the actual fire situations. The total smoke produced after burning was not substantially impacted via the existence of GOs, a significant benefit, associated with a standard flame-resistant, that boosted the optical smoke density, which represents a serious fire hazard.

In addition, it was shown that the inclusion of GO did not impact on surface charring. Actually, the development of a strong, compact and permanent char during combustion of polymer nanocompounds is a well-known impact of high-aspect nanoparticles that are well dispersed. The GO loading enabled the development of a carbonaceous protective layer obtained as a result of the polymer ablation and accumulation of GOs, acting as a heat and mass transfer barrier layer [18] that decreased the overall combustion process. The processes of fire-retardants occurred during combustion in the condensed phase through the creation of a graphene residue sheet.

A pronounced afterglow and residue thermo-oxidation took place after flame-out. For PP and its nanocomposites with graphene, the efficient heat of combustion was comparable, showing the lack of any appropriate flame-retardant mechanism in the gas phase. It had been previously noted the beneficial impact of enhancing particles' spread on the quality of the residual protective layers for carbon nanotubes [13] or epoxy/layered silicate [46].

It was found that both the macroscopic and the microscopic scale required a closed charred layer to achieve efficient flame-retardants by nanocomposites. For the functioning and effectiveness of GO residue as just a thermal barrier and shield toward mass transport, a closed and safe residue surface on top of the burning sample is crucial. It can postpone heat transport from the flame to the polymer nanocompounds, resulting in a lower temperature rise within the nanocomposite [43]. The barrier layers are functioned as the thermal transport obstacles in the deeper areas of the sample. In the neat PP and PP/GO nanocomposites, degradation of PP began at 428–450 °C. The capacity to create strong protective sheets and to operate like efficient fire-retardant fillers is regulated via dispersing nanoparticles in the polymer matrix which were seen in various carbon nanotubes and varying layered silicates on the surface of the particles [51, 52].

Figure 5 displays the images of the char residues of PP and its nanocompounds. After pristine PP burning, there was no char remained in the aluminum foil. Char characteristics with flame-resistant characteristics played important roles. All specimens had a compact and cohesive function. The white and black areas were detected in the PP char. Most bubble-like chars were produced in the char residues of the PP/GO 0.5 wt% and PP/GO 1.0 wt% nanocomposites.

Swelling degree of char for PP/GO 0.5 wt% and PP/GO 1.0 wt% was greater than that of the neat PP, indicating that low GO loading facilitates char development. Moreover, PP/GO 2.0 wt% and PP/GO 5.0 wt% nanocomposites did not show any significant enhancement in expansion. The exterior and inner parts of the char created a closed chamber. In the PP/GO 1.0 wt% nanocomposite, the hollow structure was more prominent and this type of char presented outstanding hindrance efficiency.

The graphene-enhanced exterior char must have sufficient thermal steadiness and mechanical strength to withstand combustion destruction and release gases. The compact charred intumescent layers filled with graphene were resulted for various chars of the PP/GO nanocompounds, proving that the graphene nanosheets network structure played a very significant role in the development of the strong intumescent chars during the burning of the nanocompounds which offered a great strength throughout the pyrolysis and burning. Adding GO raised the PP/GO chars carbon content. Moreover, the PP/GO char's carbon content was massive. The carbon content indicated the degree of accumulation and cross-linking: greater carbon content, greater carbon atoms per unit region in the char layer, and greater the cross-linking degree [37]. The degree of char cross-linking and char strength of chars for PP/GO were, therefore, high due to the impacts of GO nanosheets during the development of chars, which was verified by SEM analysis.

After studies with cone calorimetry, Raman spectroscopy was utilized for analyzing the graphitization level of the char residues. Char with a greater degree of graphitization often has a higher resistance to thermal oxidation, useful to improve the polymer's flame-retardants [45]. Char's Raman spectra are shown in Fig. 6. There are two primary distinctive bands of Raman spectra in Fig. 6 as D and G bands at about 1370 and 1590 cm^{-1}, correspondingly. G-band is the first-order scattering of E_{2g} vibration mode [41], and D-bands are distorted graphite or glassy carbon [18]. The degree of graphitization is determined by the proportion of the D and G bands embedded intensity (ID/IG). Peak fitting is performed with Lorentzian variety; the integrated D-to-G-band intensity ratio (*ID*/*IG*) is an indication of the degree of carbonaceous material graphitization. The greater ID/IG ratio shows the reduced degree of graphitization.

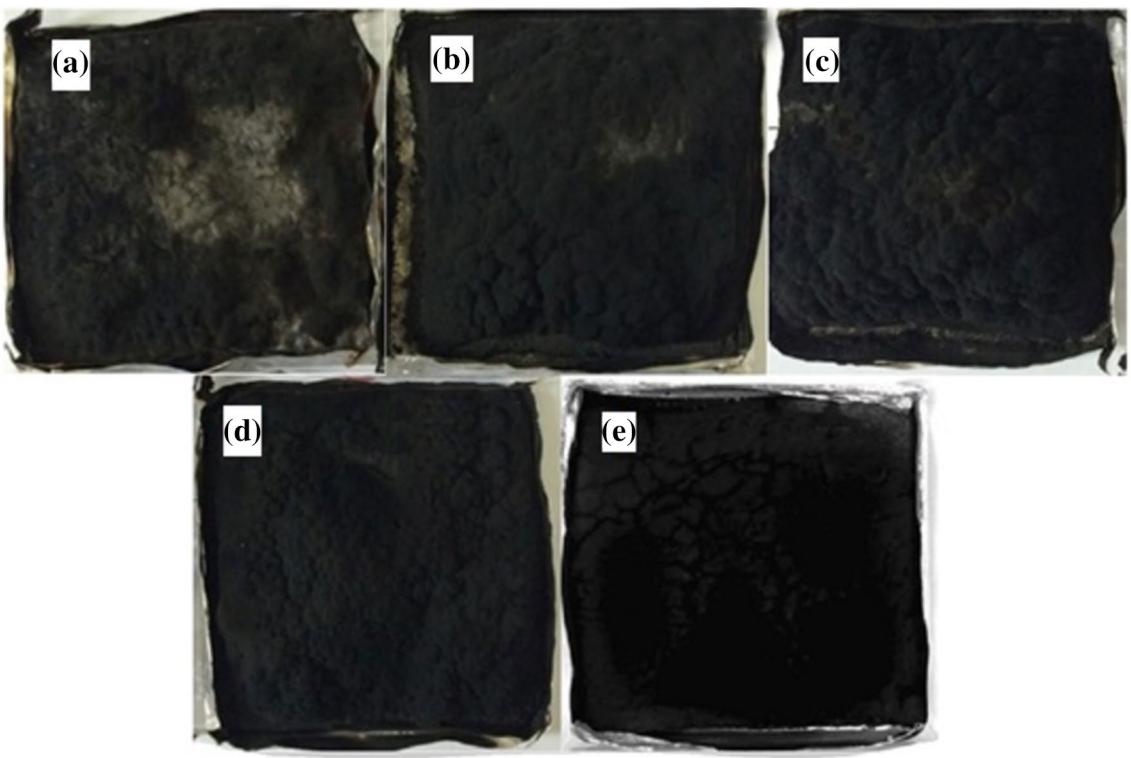

Fig. 5 Photos of deposit chars of flame-resistant PP/GO nanocomposites after cone calorimeter experiments of **a** neat PP, **b** PP/GO 0.5 wt%, **c** PP/GO 1.0 wt%, **d** PP/GO 2.0 wt%, and **e** PP/GO 5.0 wt% samples

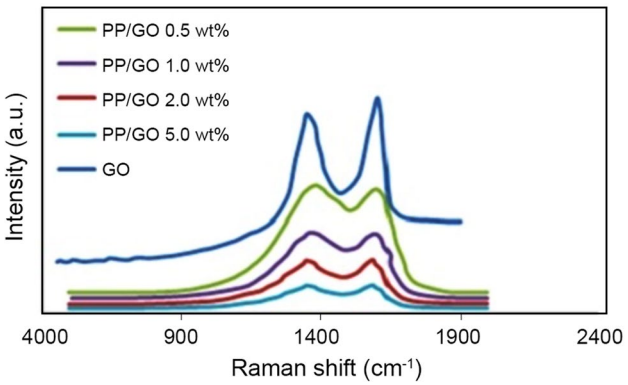

Fig. 6 Raman spectra of char layers of neat PP and PP/GO nanocomposites after cone calorimetry

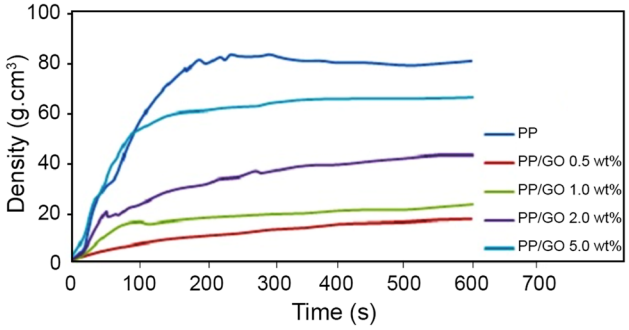

Fig. 7 Smoke densities of neat PP and PP/GO nanocomposites under flaming combustion

As shown in Fig. 6, because of the existence of amorphous carbon in forming carbon nanofibers, the rate of ID/IG for PP/GO samples was higher than that for the pristine PP. The in-situ carbon nanofibers coating on GO nanosheets improved hindrance role, leading into the more marked fire-retardants. The reduced ID/IG ratio implies a greater degree of graphitization for carbonaceous products. For greater graphitization degree of the char [42], greater thermal steadiness and greater protection of the char layer would be accomplished.

It is evident from Raman spectra that the graphitization level of the char raised with a rise in graphene loading. This can be clarified by the reality that the char layer contained more graphene residues due to increase in the GO load. Figure 6 indicates that the PP/GO 5.0 wt% specimen showed the highest and the PP/GO 0.5 wt% specimen displayed the lowest graphitization level. Graphene nanosheets can serve as a template to enhance the char's graphical order [43]. It is remarkable that in the spectrum of PP/GO 2.0 wt%, the change of D and G bands is noted, indicating an appropriate graphical structure.

Graphene's barrier impact can decrease the volatility materials available for char development, which is useful in developing a compact and thick char layer [44]. Some marked variations were observed in the PP/GO spectra, as compared the PP specimen with the one that had 1.0 wt% GO. The graphene nanosheets in the PP/GO system can act as a helpful barrier and stop volatile products from escaping, making more compounds available for char formation. The nanosheets of graphene can strengthen the layers of the intumescent developed char. Compact, thick and thermostable char has a great performance barrier and isolates the underlying materials from the flame area.

Polymer's fire hazard involves its flammability and fire effluent toxicity. During combustion, the smoke release makes extra injuries and visual obscuration, which is dangerous to run away and save a life. Smoke suppression of polymer is, therefore, of excellent importance.

The smoke density chamber was used for investigating the behavior of smoke emission in this study. Under the flaming combustion scenario, Fig. 7 displays, smoke emission analysis of PP and its nanocomposites. The smoke was discharged quickly after ignition during the burning of PP and then the trend of Fig. 7 indicates a stable rate. The smoke density rose slowly for PP and its smoke was reduced after 220 s. The intumescent char layer created can efficiently prevent the emission of smoke. Remarkably, the incorporation of 0.5–5.0 wt% of GO for the prepared nanocompounds was contributed to the further removal of the smoke. This is clarified that GO nanosheets augmented the barrier impact of the deposit char, examined by the char residue SEM observation. The PP/GO 0.5 wt% nanocomposite showed the highest efficiency in smoke removal. However, specimens of PP/GO 1.0 wt% to 5.0 wt% had the greater smoke density than the specimen PP/GO 0.5 wt%. These findings may be due to the enhanced barrier impact relevant to the elevated GO loading which led to a deficiency of oxygen, incomplete combustion and more smoke generation [52]. The graphene, as a flame-resistant for PP, revealed suitably as a smoke suppression factor.

One of the main variables influencing the growth of the intumescent char layer is the melt viscosity of the polymer components. Melt viscosity was evaluated by the MFI test, which is indirectly relative to the polymer melt viscosity. Figure 8 shows the MFI rates of the PP and its nanocomposites at different temperatures and varying GO content. The rising temperature by heating resulted in the increase in the MFI values, indicating enhanced mobility of the melted liquid. A suddenly lowered MFI at 285 °C was noted for the pristine PP specimen that is owing to the oxidation cross-linking reaction that reduced the melt mobility [53]. Rigid graphene nanofiller can enhance polymer matrix melt viscosity by developing a network [54].

As shown in Fig. 8, further inclusion of GO from 0.5–5.0 wt% gradually reduced PP's MFI values at each temperature.

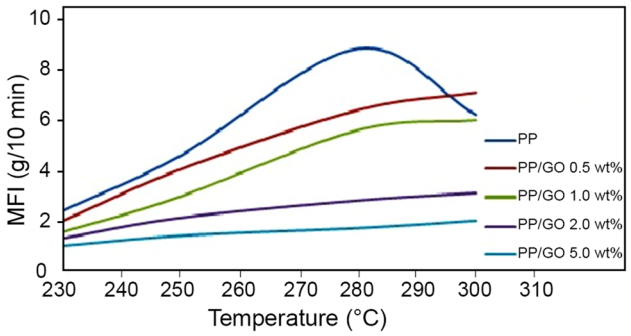

Fig. 8 Variation of melt flow index of neat PP and PP/GO nanocomposites vs. temperature

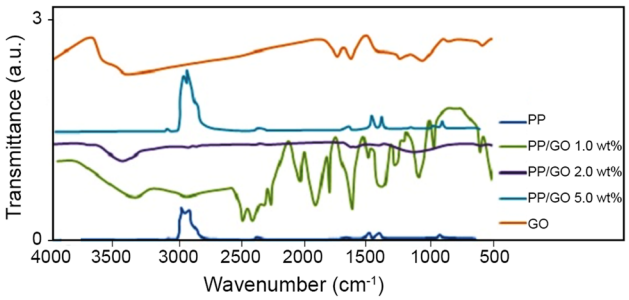

Fig. 9 FTIR spectra of char residue of neat PP and PP/GO nanocomposites

In UL-94 and LOI experiments, the rise in melt viscosity due to the addition of GO nanosheets caused the anti-drip mechanism [21]. The impact of inclusion of nanomaterials caused the viscosity of the polymer melt to grow at small shear rates and this phenomenon was studied before [14, 49, 50].

The morphology of the carbon nanoparticles defined the spread of these particles in PP, with a growing distribution leading to a great melt flow alteration and rheological behavior. For well-exfoliated sheets in PP/GO 5.0 wt% sample, the impact was the most pronounced one. At the higher GO loading, the nano dispersed carbon nanoparticles act as an anti-dripping agent without significantly affecting processes at higher shear rates (Fig. 8). The governing variables influencing the extinction of polymers are the flammability experiments with a small flame, melt viscosity, dripping property, and incombustible gas discharge [54].

Analysis of PP and PP/GO nanocomposites condensed and gaseous phase thermal degradation materials were performed by FTIR. The emitted gas products of PP and PP/GO nanocomposites showed characteristic bands of saturated hydrocarbons (2964, 2919, 1468, 1379, 1148 and 969 cm^{-1}), unsaturated alkane (3078, 1622 and 890 cm^{-1}) and CO_2 (2366 and 2318 cm^{-1}) [11, 13]. It can be noted that PP degradation products at the first peak level of decomposition are comparable to PP/GO nanocompounds with 1.0 wt% GO content. This study showed that GO worked like inert filler and did not affect PP's path of thermal decomposition. Though, at the second peak rate, CO_2 signals in the spectrum of PP/GO 1.0 wt% was vanished. Graphene oxide nanosheets delayed the release of volatile degradation materials because of the spread and outstanding barrier structure.

Char residues were explored with FTIR, as shown in Fig. 9, to determine functional groups. Two peaks ascribing to C–H for PP are noted at 2926 and 2858 cm^{-1} for the FTIR range of PP/GO 1.0 wt% specimen due to superior GO thermal-oxidative stability. Thermal degradation of PP happens within 360–495 °C in a single step, which no residue is left after the experiment. Identified signals of PP pyrolysis outcomes are C–H and C–C single and double bonds of $–CH_3$, $–CH_2–$ and CH_2 groups. Signals associated with $–CH_3$ were noticed at 2960 cm^{-1}, 2875 cm^{-1}, 2733 cm^{-1}, 1460 cm^{-1}, 1379 cm^{-1}, 1150 cm^{-1}, 969 cm^{-1} and 806 cm^{-1}. Signals associated with $–CH_2$ were at 2920 cm^{-1} and 2850 cm^{-1}; signals ascribed to CH_2 were identified at 3079 cm^{-1}, 1785 cm^{-1}, 1645 cm^{-1} and 887 cm^{-1}.

Structural classes identified as $–CH_3$, $–CH_2–$ and CH_2, showed the degradation of typical PP via development of aliphatic and olefin degradations [44, 45]. The addition of 5.0 wt% GO to PP did not alter the type of pyrolysis outcomes which resulted in detection of the same FTIR signals. GO's spectrum is shown in Fig. 9. GO displayed the characteristic of CO, COC, and COH groups at about 1730, 1220 and 1048 cm^{-1} [25, 26], correspondingly.

Figure 9 demonstrates remaining char FTIR spectra that provide data about the residue chemical structure. The peaks at about 1628 cm^{-1} and 1581 cm^{-1} are from the absorption of moisture and/or characteristic peak of graphene [24]. The presence of 1108 cm^{-1} peak for CO bonds supported the oxidation of graphene through combustion in a cone calorimeter experiment. The reduction in the intensity of oxygen functional groups of GO is indicative of its reduction throughout preparation reaction. The existence of 1108 cm^{-1} peak for CO bonds verified oxidation of graphene via combustion in the cone calorimeter experiment. For GO, the bands at 1719, 1225 and 1053 cm^{-1} are the characteristic peaks of COOH, COC, and COH, correspondingly [17, 22].

Figure 10a–e exhibits the spreading of GO in the polymer matrix observed by SEM. They deliver micrometer-scale graphene spreading information. The SEM micrographs of the PP/GO nanocomposite show massive GO agglomerates. The GO nanosheets were generally uniformly spread in the matrix, although some of them were detected to be restacked. Following combustion, morphology and char structure were studied with SEM to explain how char formation would impact on the PP/GO nanocomposite combustion.

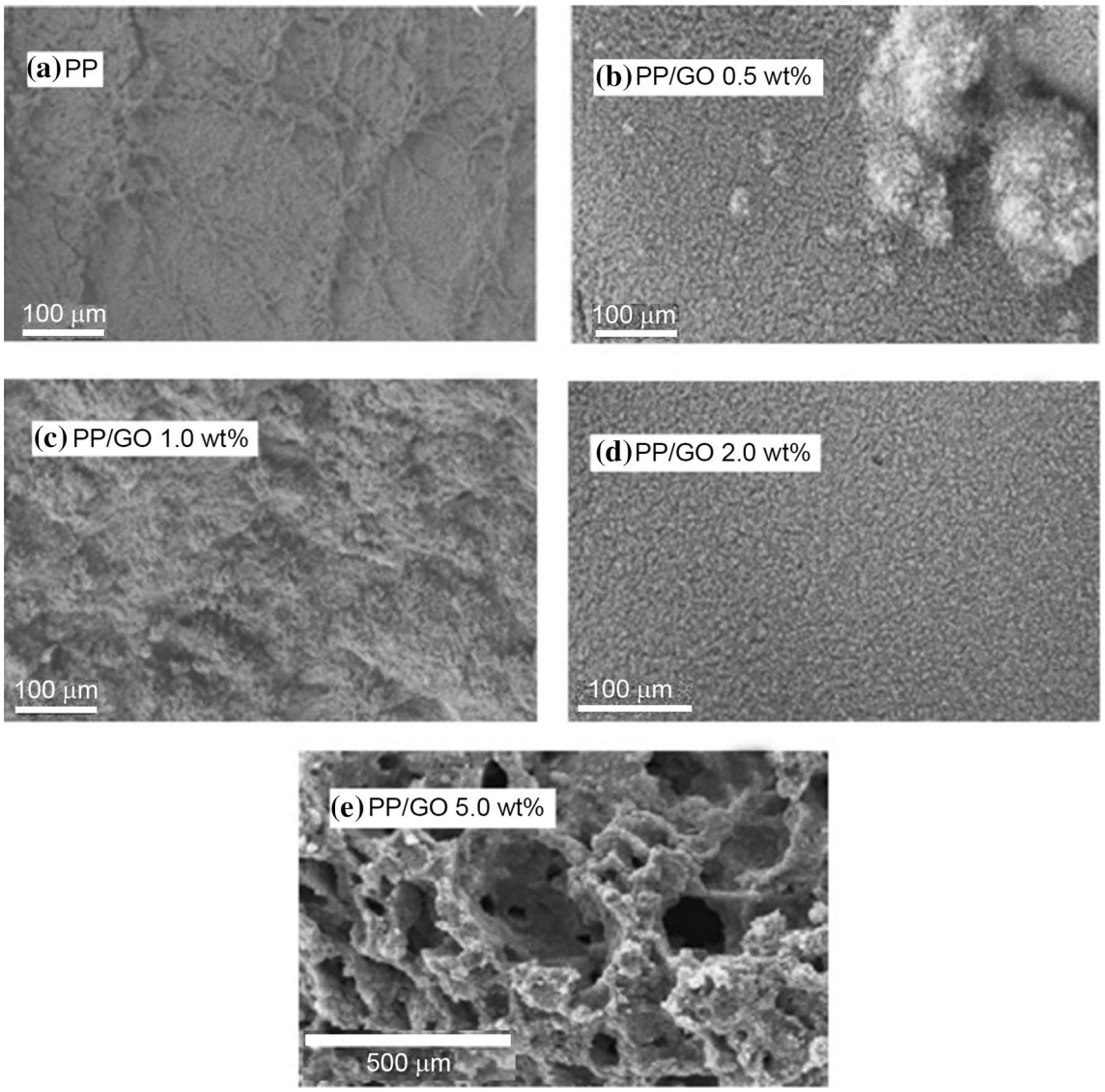

Fig. 10 SEM micrographs of char layers after cone calorimetry: **a** neat PP, **b** PP/GO 0.5 wt%, **c** PP/GO 1.0 wt%, **d** PP/GO 2.0 wt%, and **e** PP/GO 5.0 wt% samples

Figure 10a–e demonstrates the remaining char SEM micrographs after combustion for PP/GO nanocomposites. Figure 10a–e reveals some exfoliated graphene nanosheets, enclosed with a small number of carbonaceous particles forming barriers and protective shields in PP/GO chars on the residue surface of the samples that prevented heat diffusion and transmission, while they were subjected to flames or heat sources.

Figure 11 shows the GO and PP/GO nanocomposites TEM images. Figure 11a characterizes the dispersal status of the GO nanosheets in the matrix. It provides micrometer-scale of GO nanosheets data displaying their massive agglomerates in the PP/GO nanocomposites. The PP/GO nanocomposite TEM images (Fig. 11b, c) indicate a principally exfoliated structure with an amount of noticeable individual GO nanosheets, following previous findings on other polymers/graphene nanocomposites [2, 11, 15]. In high-magnification TEM image (Fig. 11c) aligned graphene nanosheets look as separate dark lines. Due to structural defects, GO's TEM images demonstrated layered, crumpled, and wrinkled morphology (Fig. 11). The GO was distributed as aggregates in the matrix. The distribution or agglomeration of the nanofillers relies on their length within the polymer matrix [40].

Conclusion

The PP/GO nanocomposites, filled with 0.5–5.0 wt% GO were able to achieve the UL-94 without dripping and V-1 rate. In comparison with PP, the PHRR value of the PP/GO

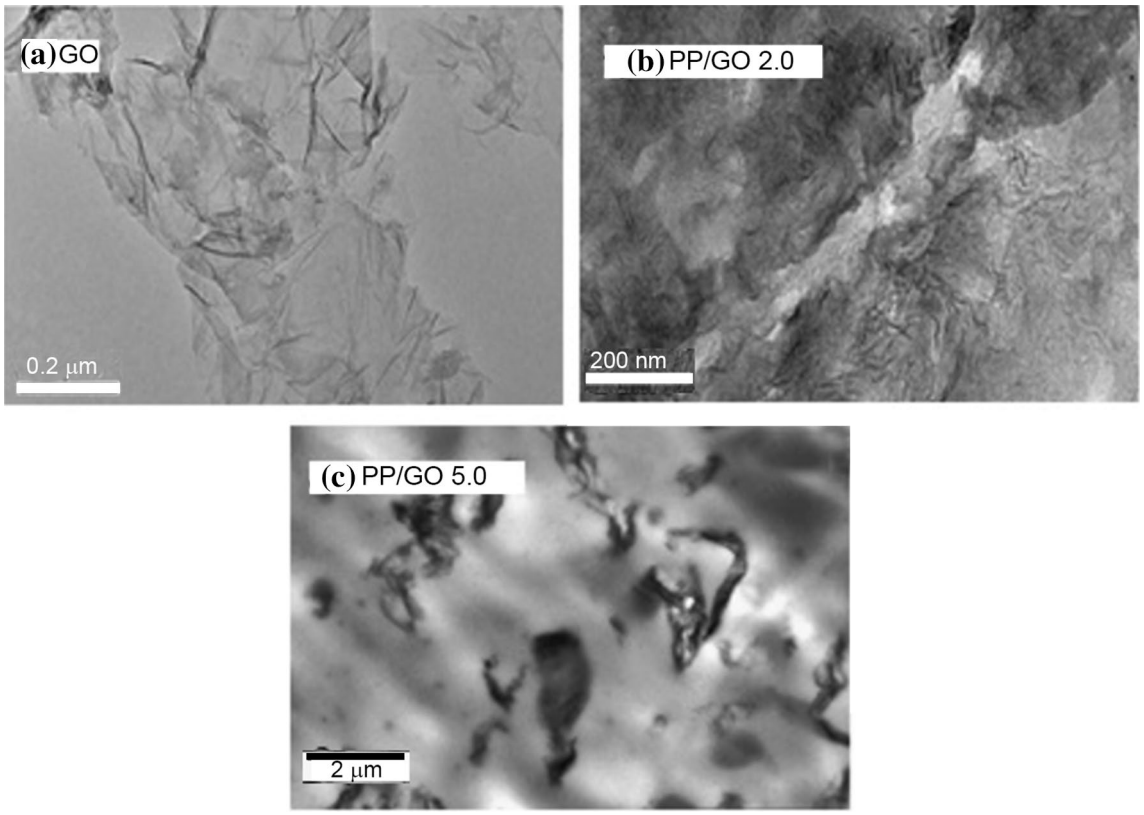

Fig. 11 TEM micrographs of **a** GO, **b** PP/GO 2.0 wt% and **c** PP/GO 5.0 wt% samples

nanocompounds lowered to 78%. TGA test outcomes presented that inclusion of GO into PP enhanced meaningfully the thermal steadiness due to the formation of compressed intumescent char verified with SEM micrographs. GO load (0.5–5.0 wt%) in PP decreased PHRR values from 1140 to 620 kW m^{-2}. Graphene oxide loading maintained LOI values statistically unchanged, but promoted the UL-94 rating at the same time. As a result of a well-dispersed GO in the PP matrix, PP/GO nanocompounds showed a higher thermal degradation point and large alterations in the rheological behavior of the melting polymer. Owing to the increased heat conductivity for PP/GO nanocomposites, the neat PP showed a reduction in the time for ignition. During combustion, the residue layer development shielded the underlying polymer and decreased PHRR to 78%. The macroscopic and microscopic constructions of the deposited char showed that inclusion of GO reinforced the compactness of PP/GO nanocomposites which make them flame-resistant.

References

1. Ajorloo M, Fasihi M, Ohshima M, Taki K (2019) How are the thermal properties of polypropylene/graphene nanoplatelet composites affected by polymer chain configuration and size of nanofiller. Mater Des 181:108068
2. Yuan B, Fan A, Yang M, Chen X, Hu Y, Bao C, Jiang S, Niu Y, Zhang Y, He S, Dai H (2017) The effects of graphene on the flammability and fire behavior of intumescent flame-resistant polypropylene composites at different flame scenarios. Polym Degrad Stabil 143:42–56
3. Papageorgiou DG, Terzopoulou Z, Fina A, Cuttica F, Papageorgiou GZ, Bikiaris DN, Chrissafis K, Young RJ, Kinloch IA (2018) Increased thermal and fire retardancy properties of polypropylene reinforced with a hybrid graphene/glass-fibre filler. Compos Sci Technol 156:95–102
4. Yan L, Zhisheng X, Deng N (2020) Synthesis of organophosphate-functionalized graphene oxide for enhancing the flame retardancy and smoke suppression properties of transparent fire-retardant coatings. Polym Degrad Stabil 172:109064
5. Yuan B, Hu Y, Chen X, Shi Y, Niu Y, Zhang Y, He S, Dai H (2017) Dual modification of graphene by polymeric flame resistant and $Ni(OH)_2$ nanosheets for improving flame retardancy of polypropylene. Compos Part A Appl Sci Manuf 100:106–117
6. Yuan B, Wang B, Hu Y, Mu X, Hong N, Liew KM, Hu Y (2016) Electrical conductive and graphitizable polymer nanofibers grafted on graphene nanosheets: improving electrical conductivity and flame retardancy of polypropylene. Compos Part A Appl Sci Manuf 84:76–86
7. Li Z, González AJ, Heeralal VB, Wang D-Y (2018) Covalent assembly of MCM-41 nanospheres on graphene oxide for improving fire retardancy and mechanical property of epoxy resin. Compos B Eng 138:101–112
8. Papageorgiou DG, Terzopoulou Z, Fina A, George FC, Papageorgiou Z, Bikiaris DK, Chrissafis K, Young RJ, Kinloch IA (2018)

Increased thermal and fire retardancy properties of polypropylene reinforced with a hybrid graphene/glass-fibre filler. Compos Sci Technol 156:95–102
9. Sabet M, Soleimani H (2017) The impact of electron beam irradiation on low density polyethylene and ethylene vinyl acetate. IOP Conf Ser Mater Sci Eng 204:012005
10. Xu W, Liang B, Xiaoling Z, Guisong W, Ding WD (2018) The flame retardancy and smoke suppression effect of a hybrid containing CuMoO4 modified reduced graphene oxide/layered double hydroxide on epoxy resin. J Hazard Mater 343:364–375
11. Sabet M, Soleimani H (2019) Broad studies of graphene and low-density polyethylene composites. J Elastom Plast 51:527–561
12. Feng Y, He C, Wen Y, Ye Y, Zhou X, Xie X, Mai YW (2018) Superior flame retardancy and smoke suppression of epoxy-based composites with phosphorus/nitrogen co-doped graphene. J Hazard Mater 346:140–151
13. Yuan B, Fan A, Yang M, Chen X, Hu Y, Bao C, Jiang S, Niu Y, Zhang Y, He S, Dai H (2017) The effects of graphene on the flammability and fire behavior of intumescent flame resistant polypropylene composites at different flame scenarios. Polym Degrad Stabil 143:42–56
14. Sabet M, Soleimani H, Hassan A, Ratnam CT (2014) Electron beam irradiation of LDPE filled with calcium carbonate and metal hydroxides. Polym Plast Technol Eng 53:1362–1366
15. Feng Y, He C, Wen Y, Ye Y, Zhou X, Xie X, Mai Y-W (2017) Improving thermal and flame resistant properties of epoxy resin by functionalized graphene containing phosphorous, nitrogen and silicon elements. Compos Part A Appl S 103:74–83
16. Sabet M, Hassan A, Ratnam CT (2013) Properties of ethylene–vinyl acetate filled with metal hydroxide. J Elastom Plast 47:88–100
17. Xu W, Zhang B, Xu B, Li A (2016) The flame retardancy and smoke suppression effect of heptaheptamolybdate modified reduced graphene oxide/layered double hydroxide hybrids on polyurethane elastomer. Compos Part A Appl S 91(Part 1):30–40
18. Zhao Z, Cai W, Xu Z, Mu X, Ren X, Zou B, Gui Z, Hu Y (2020) Multi-role p-styrene sulfonate assisted electrochemical preparation of functionalized graphene nanosheets for improving fire safety and mechanical property of polystyrene composites. Compos Part B Eng 181:107544
19. Li Y, Liu J, Wang S, Zhang L, Shen B (2020) Self-templating graphene network composites by flame carbonization for excellent electromagnetic interference shielding. Compos Part B Eng 182:107615
20. Soleimani H, Yahya N, Baig MK, Khodapanah L, Sabet M, Burda M, Oechsner A, Awang M (2015) Synthesis of carbon nanotubes for oil-water interfacial tension reduction. Oil Gas Res 1:104. https://doi.org/10.4172/2472-0518.1000104
21. Qu L, Sui Y, Zhang C, Li P, Dai X, Xu B, Fang D (2020) POSS-functionalized graphene oxide hybrids with improved dispersive and smoke-suppressive properties for epoxy flame-retardant application. Eur Polym J 122:109383
22. Soleimani H, Latiff NRA, Yahya N, Sabet M, Khodapanah L, Kozlowski G, Chuan LK, Guan BH (2016) Synthesis and characterization of yttrium iron garnet (YIG) nanoparticles activated by electromagnetic wave in increased oil recovery. J Nano Res 38:40–46
23. Sabet M, Hassan A, Ratnam CT (2013) Electron-beam irradiation of low-density polyethylene/ethylene vinyl acetate blends. J Polym Eng 33:149–161
24. Sabet M, Soleiman H, Hosseini S (2019) Thermal and flammable stability of radiated LDPE and composites. Int J Plast Technol 23:239–245
25. Sabet M, Soleimani H, Hosseini S (2018) Effect of addition graphene to ethylene vinyl acetate and low-density polyethylene. J Vinyl Addit Technol 24:E177–E185
26. Xiao Y, Jin Z, He L, Ma S, Wang C, Mu X, Song L (2020) Synthesis of a novel graphene conjugated covalent organic framework nanohybrid for enhancing the flame retardancy and mechanical properties of epoxy resins through synergistic effect. Compos Part B Eng 182:107616
27. Li L, Liu XL, Shao X, Jiang L, Huang K, Zhao S (2020) Synergistic effects of a highly effective intumescent flame-retardant based on tannic acid functionalized graphene on the flame retardancy and smoke suppression properties of natural rubber. Compos Part A Appl S 129:105715
28. Sabet M, Soleimani H, Mohammadian E (2019) Effect of graphene and carbon nanotube on low-density polyethylene nanocomposites. J Vinyl Addit Technol 25(1):35–40
29. Feng Y, Han G, Wang B, Zhou X, Ma J, Ye Y, Liu C, Xie X (2020) Multiple synergistic effects of graphene-based hybrid and hexagonal born nitride in enhancing thermal conductivity and flame retardancy of epoxy. Chem Eng J 379:122402
30. Sabet M, Soleimani H (2018) Thermal, electrical and characterization effects of graphene on the properties of low-density polyethylene composites. Int J Plast Technol 22:234–246
31. Du W, Jin Y, Lai S, Shi L, Shen Y, Yang H (2020) Multifunctional light-responsive graphene-based polyurethane composites with shape memory, self-healing, and flame retardancy properties. Compos Part A Appl S 128:105686
32. Boyd DA, Lin W-H, Hsu C-C, Teague ML, Chen C-C, Lo Y-Y, Chan W-Y, Su W-B, Cheng T-C, Chang C-S, Wu C-I, Yeh N-C (2015) Single-step deposition of high-mobility graphene at reduced temperature. Nat Commun 6:6620. https://doi.org/10.1038/ncomms7620
33. Sabet M, Hassan A, Ratnam CT (2013) Effect of zinc borate on flammability/thermal properties of ethylene vinyl acetate filled with metal hydroxides. J Reinf Plast Compos 32:1122–1128
34. Kaindl R, Jakopic G, Resel R, Pichler J, Fian A, Fisslthaler E, Grogger W, Bayer BC, Fischer R, Waldhauser W (2015) Synthesis of graphene-layer nanosheet coatings by PECV. Mater Today 2:4247–4255
35. Zhou K, Gao R (2017) The influence of a novel two-dimensional graphene-like nanomaterial on thermal steadiness and flammability of polystyrene. J Colloid Interface Sci 500:164–171
36. Sabet M, Soleimani H, Hosseini S (2016) Properties and characterization of ethylene-vinyl acetate filled with carbon nanotube. Polym Bull 73:419–434
37. Ji Y, Li Y, Chen G, Xing T (2017) Fire-resistant and highly electrically conductive silk fabrics fabricated with reduced graphene oxide via dry-coating. Mater Des 133:528–535
38. Zhou K, Gui Z, Hu Y, Jiang S, Tang G (2016) The influence of cobalt oxide–graphene hybrids on thermal degradation, fire hazards and mechanical properties of thermoplastic polyurethane composites. Compos Part A Appl S 88:10–18
39. Zhou K, Gui Z, Hu Y (2016) The influence of graphene based smoke suppression agents on reduced fire hazards of polystyrene composites. Compos Part A Appl S 80:217–227
40. Sabet M, Soleimani H (2014) Mechanical and electrical properties of low-density polyethylene filled with carbon nanotubes. IOP Conf Ser Mater Sci Eng. https://doi.org/10.1088/1757-899X/64/1/012001
41. Chen X, Ma C, Jiao C (2016) Enhancement of flame-retardant performance of thermoplastic polyurethane with the incorporation of aluminum hypophosphite and iron-graphene. Polym Degrad Stabil 129:275–285
42. Liu S, Fang Z, Yan H, Chevali VS, Wang H (2016) Synergistic flame retardancy effect of graphene nanosheets and traditional retardants on epoxy resin. Compos Part A Appl S 89:26–32
43. Herki BMA (2017) Combined effects of modified polystyrene and unprocessed fly ash on concrete characteristics produced by a novel technique of densification. World Eng Appl Sci J 8:118–129

44. Sabet M, Soleiman H (2020) Graphene impact on thermal characteristics of LDPE. Polym Sci Ser A 61:922–930
45. Vijayasarathi P, Suresh Prabhu P, Rajaram G (2015) Investigation of composite coated Ti-C-N surfaces with ball-cratering test method. Carbon Sci Technol 7:30–36
46. Hosseini SN, Shuker MT, Sabet M, Zamani A, Hosseini Z, Shabib AA (2015) Brine ions and mechanism of low salinity water injection in enhanced oil recovery: a review. Res J Appl Sci Eng Technol 11:1257–1264
47. Liu Y, Lu M, Hu Z, Liang L, Shi J, Huang X, Lu M, Wu K (2020) Casein phosphopeptide-biofunctionalized graphene oxide nanoplatelets based cellulose green nanocomposites with simultaneous high thermal conductivity and excellent flame retardancy. Chem Eng J 382:122733
48. Rahimi-Aghdam T, Shariatinia Z, Hakkarainen M, Haddadi-Asl V (2020) Nitrogen and phosphorous doped graphene quantum dots: excellent flame-retardants and smoke suppressants for polyacrylonitrile nanocomposites. J Hazard Mater 381:121013
49. Zhou S, Ning M, Wang X, Yan Z, Guo D, He Q, Zhang Y, She S, Hu Y (2014) The influence of γ-radiation on the mechanical, thermal decomposition, and flame retardant characteristics of EVA/LDPE/ATH blends. J Therm Anal Calorim 119:167–173
50. Zhang M, Ding X, Zhan Y, Wang Y, Wang X (2020) Improving the flame retardancy of poly (lactic acid) using an efficient ternary hybrid flame-retardant by dual modification of graphene oxide with phenylphosphinic acid and nano MOFs. J Hazard Mater 384(15):121260
51. Sabet M, Syafiq M (2013) Calcium stearate and alumina trihydrate addition of irradiated LDPE, EVA and blends with electron beam. Appl Mech Mater 290:31–37
52. Eshkalak KE, Sadeghzadeh S, Jalaly M (2020) Thermal resistance analysis of hybrid graphene-boron nitride nanosheets: the effect of geometry, temperature, size, strain and structural defects. Comput Mater Sci 174:109484
53. Owais M, Zhao J, Imani A, Wang G, Zhang H, Zhang Z (2019) Synergetic effect of hybrid fillers of boron nitride, graphene nanoplatelets, and short carbon fibers for enhanced thermal conductivity and electrical resistivity of epoxy nanocomposites. Compos Part A Appl S 117:11–22
54. Sabet M, Savory RM, Hassan A, Rantam CT (2013) The effect of TMPTMA addition on electron-beam irradiated LDPE, EVA and blend properties. Int Polym Process 28:386–392
55. Sang B, Li Z-W, Li X-H, Yu L-G, Zhang Z-J (2016) Graphene-based flame-retardants: a review. J Mater Sci 51:8271–8295